


Emergent phase transitions in a cluster Ising model with dissipationZheng-Xin Guo,^{1,2,*} Xue-Jia Yu,^{3,*} Xi-Dan Hu^{4,5}  and Zhi Li^{1,†}¹*Guangdong-Hong Kong Joint Laboratory of Quantum Matter, Frontier Research Institute for Physics, South China Normal University, Guangzhou 510006, China*²*Wilczek Quantum Center and Key Laboratory of Artificial Structures and Quantum Control, School of Physics and Astronomy, Shanghai Jiao Tong University, Shanghai 200240, China*³*International Center for Quantum Materials, School of Physics, Peking University, Beijing 100871, China*⁴*Guangdong Provincial Key Laboratory of Quantum Engineering and Quantum Materials, SPTE, South China Normal University, Guangzhou 510006, China*⁵*GPETR Center for Quantum Precision Measurement, South China Normal University, Guangzhou 510006, China*

(Received 15 March 2022; accepted 17 May 2022; published 27 May 2022)

We study a cluster Ising model with non-Hermitian external field which can be exactly solved in the language of free fermions. By investigating the second derivative of energy density and fidelity, the possible new critical points are tentatively located. The string order parameter and staggered magnetization are then detected to reveal emergent phases of brand new characteristics. To categorize the exotic phases and phase transitions induced by non-Hermiticity, we calculate the variation mode of the spin-correlation function as well as of the string correlation function, which characterize the emergent phases and critical points with different patterns of decay and critical exponents. With the help of the string order parameter and staggered magnetization, we find that there are four phases after introducing the non-Hermiticity—the cluster phase, the gapless phase, the paramagnetic phase, and the antiferromagnetic phase. A phase diagram is then presented to graphically illustrate, based on two “Kosterlitz-Thouless-like” phase transitions and an Ising phase transition, respectively, the generation of three critical lines as non-Hermitian strength increases. Our theoretical work is expected to be realized in the experiment of ultracold atoms, pushing for progress in exploring novel phases and phase transitions.

DOI: [10.1103/PhysRevA.105.053311](https://doi.org/10.1103/PhysRevA.105.053311)**I. INTRODUCTION**

According to the conventional Landau-Ginzberg-Wilson paradigm [1], an ordered phase is characterized by certain symmetry breaking of the system, whereas a disordered phase features the preservation of symmetry. The phase transition between ordered phases and disordered phases can be detected by certain local parameters. However, Kosterlitz and Thouless discovered a continuous phase transition without symmetry breaking in systems involving classical vortex topology, which is named the Kosterlitz-Thouless (KT) phase transition [2]. The key characteristic of a KT phase transition is that it occurs between a disordered phase and a gapless phase with quasi-long-range order which can be detected by the power-law decay of the correlation function.

With the rapid development of quantum simulation and computation, the marriage of traditional condensed-matter physics and cutting-edge experimental techniques gives birth to various new topics. In highly pure and controllable ultracold atom platforms, a triangle optical lattice can be set up with atoms loaded in a unique way [3] so as to create an equivalent three-spin ring-exchange interaction in a spin system that can be mapped to a “zigzag chain.”

Notably, the ground state of the system is a cluster state [4], a disordered state whose spin spatial rotational symmetry is protected. However, research also indicates that except for a three-spin ring interaction, a two-spin interaction relating to the symmetry-breaking state is also observed in such a system, causing competition between the two kinds of interactions. From the view of quantum information, researchers regard the two-spin interaction as a perturbation, for it will damage the symmetry-protected topological (SPT) cluster state, and they are curious about the SPT threshold of robustness [5–10]. From the perspective of condensed-matter physics, the exotic continuous quantum phase transitions (QPTs) between the SPT phases and symmetry-breaking phases are fascinating for their own sake [11–13]. Therefore, the cluster Ising model is put forward as a good toy model to investigate the phase transitions in such quantum many-body systems. Generally, the SPT cluster phase is protected by a $\mathbb{Z}_2 \times \mathbb{Z}_2$ symmetry [14] and can be characterized by nonlocal string order [15,16], while the symmetry-breaking antiferromagnetic (AFM) state can be identified by local staggered magnetization [17,18].

The above discussion is based on traditional quantum mechanics, which requires the Hermiticity of observables to ensure that their eigenvalues are real numbers. However, non-Hermitian physics has currently attracted extensive research interest as the non-Hermitian experimental techniques mature in a wide range of tabletop experimental platforms [19,20], including the ultracold atom system [21,22],

*These authors contributed equally.

†lizphys@m.scnu.edu.cn

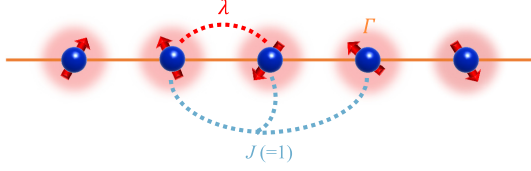


FIG. 1. Graphic demonstration of the cluster Ising model with dissipation, where λ/J is the ratio of Ising exchange strength to cluster exchange strength and Γ is the strength of loss or gain. We take $J = 1$ in the following discussion.

optical system [23–26], nitrogen-vacancy center [27], etc. Many novel non-Hermitian phenomena have been detected, such as parity-time (\mathcal{PT}) symmetry [28–30], non-Hermitian skin effect [31,32], new topological behaviors associated with exceptional points [20,33–38], disorder induced by non-Hermiticity [39–42], etc. Recently, much attention has been paid to how non-Hermiticity influences quantum phase transitions in systems with rotation-time-reversal (\mathcal{RT}) symmetry [42–46], spin model with imaginary external field [47–51], and so on. It is also worth mentioning that some researchers have developed a non-Hermitian linear response theory, which uses dissipation as a means to reveal the properties of a Hermitian equilibrium system [52].

In this work, we try to uncover the connection between novel emergent phases and non-Hermiticity without \mathcal{PT} or \mathcal{RT} symmetry. The main body of this paper is organized as follows. In Sec. II, we introduce the cluster Ising model with on-site dissipations and analytically transform it into a free fermion expression. In Sec. III, the observables and the methods we adopted to characterize quantum phase transitions are presented. In Sec. IV, we give the theoretical results of observables and discuss the exotic phase diagram and phase transitions. We summarize our work in Sec. V.

II. MODEL AND EXACT SOLUTION

In this section, we establish the non-Hermitian cluster Ising model and conduct the diagonalization procedure to obtain an exact solution of the ground state. Based on the conventional cluster Ising model, we build up our Hamiltonian by inserting dissipation, which is equivalent to an external imaginary field. The expression reads

$$H = -J \sum_{l=1}^N \sigma_{l-1}^x \sigma_l^z \sigma_{l+1}^x + \lambda \sum_{l=1}^N \sigma_l^y \sigma_{l+1}^y + \frac{i\Gamma}{2} \sum_{l=1}^N \sigma_l^u, \quad (1)$$

where σ_l^x , σ_l^y , and σ_l^z are Pauli matrices of the l th spin and σ^u denotes the matrix $\begin{bmatrix} 1 & 0 \\ 0 & 0 \end{bmatrix}$ corresponding to the loss or gain, which is a simple way to involve non-Hermiticity in optical or atomic experiments [24,40,53,54]. N is large enough for us to view $N/2$ as a “decent half” regardless of the parity of N . There are three control parameters J , λ , and Γ in our model, where the former two indicate the competition between the SPT phase and symmetry-breaking phase, while the latter determines the strength of the complex field (see Fig. 1). Notably, in this work, we set $J = 1$ and take it as an energy unit in the following calculations.

The diagonalization process can be divided into three steps. First of all, we rewrite the Hamiltonian in free fermionic language using the standard Jordan-Wigner transformation, which is defined as

$$\sigma_l^z = 1 - 2c_l^\dagger c_l, \quad (2)$$

$$\sigma_l^+ = \prod_{j<l} (1 - 2c_j^\dagger c_j) c_l, \quad (3)$$

where c_l^\dagger and c_l are the creation and annihilation operators at site l , respectively. Then we can obtain the Hamiltonian in a spinless fermion expression as

$$H = \sum_l^N [-c_l^\dagger - c_l](c_{l+2}^\dagger + c_{l+2}) + \lambda(c_l^\dagger + c_l)(c_{l+1}^\dagger - c_{l+1}) - \frac{i\Gamma}{2} \sum_l^N (1 - c_l^\dagger c_l). \quad (4)$$

Second, a Fourier transformation $c_l = \frac{1}{\sqrt{N}} \sum_{k=-\pi/2}^{\pi/2} e^{2\pi ikl/N} b_k$ is conducted and we have

$$H = 2 \sum_k [iy_k(c_k^\dagger c_{-k}^\dagger + c_k c_{-k}) + z_k(c_k^\dagger c_k + c_{-k}^\dagger c_{-k} - 1)]. \quad (5)$$

Here, $y_k = -\sin(2k) - \lambda \sin(k)$ and $z_k = -\cos(2k) + \lambda \cos(k) + \frac{i\Gamma}{4}$. Third, a Bogoliubov transformation helps diagonalize the above equation, which reads

$$b_k = \cos\left(\frac{\theta_k}{2}\right) \gamma_k + i \sin\left(\frac{\theta_k}{2}\right) \gamma_{-k}^\dagger, \quad (6)$$

$$b_{-k} = \cos\left(\frac{\theta_k}{2}\right) \gamma_{-k} - i \sin\left(\frac{\theta_k}{2}\right) \gamma_k^\dagger. \quad (7)$$

Eventually, a diagonalized solution is acquired as

$$H = \sum_{k>0} \Lambda_k \left(\gamma_k^\dagger \gamma_k - \frac{1}{2} \right), \quad (8)$$

where

$$\Lambda_k = \sqrt{y_k^2 + z_k^2}, \quad (9)$$

$$\tan(\theta_k) = -\frac{y_k}{z_k}, \quad (10)$$

and the ground state of the model is

$$|G\rangle = \prod_{k>0} \left[\cos\left(\frac{\theta_k}{2}\right) + i \sin\left(\frac{\theta_k}{2}\right) c_k^\dagger c_{-k}^\dagger \right] |\text{Vac}\rangle, \quad (11)$$

where $|\text{Vac}\rangle$ denotes the vacuum state of the free fermion.

III. OBSERVABLES AND METHODS

A. Ground-state energy density and its second derivative

The nonanalyticity in the second derivative of ground-state energy density implies that a continuous QPT occurs at zero temperature. According to the above solution, the ground-state energy can be calculated analytically and numerically

via the equation

$$U_g = -\frac{2}{N} \sum_{k>0} \sqrt{y_k^2 + z_k^2} = -\frac{1}{\pi} \int_0^\pi \sqrt{y_k^2 + z_k^2} dk, \quad (12)$$

and we can easily obtain the second derivative of U_g with respect to λ , i.e., $\frac{\partial^2 U_g}{\partial \lambda^2}$.

B. Fidelity

As the inner product of two wave functions with a tiny difference in parameters, fidelity is also efficient in indicating the critical points of QPTs, whose expression reads

$$F(\lambda, \lambda + \epsilon) = \langle G(\lambda) | G(\lambda + \epsilon) \rangle = \prod_{k>0} F_k, \quad (13)$$

with

$$F_k = \cos \frac{\theta_k(\lambda) - \theta_k(\lambda + \epsilon)}{2}. \quad (14)$$

It is noticeable that ϵ should take a small value. However, some arbitrariness in choosing the value of ϵ can be allowed within a reasonable range, and the selection rule is just as what we have discussed before [13]. Here, we set $\epsilon = 10^{-5}$, which can ensure the stability of results under different parameters.

C. Order parameters

Two kinds of order parameters will be investigated in this section, i.e., a nonlocal string order parameter characterizing a disordered phase, and local staggered magnetization characterizing an AFM phase. These order parameters will be nonzero as long as the system is in the corresponding phase.

Let us begin with the string order parameter, which is defined as

$$\mathcal{O}^x = \lim_{N \rightarrow \infty} (-1)^N \left\langle \sigma_1^x \sigma_2^y \left(\prod_{k=3}^{N-2} \sigma_k^z \right) \sigma_{N-1}^y \sigma_N^x \right\rangle_0. \quad (15)$$

Using the technique in Ref. [55], we can express it by the product of $A_j = c_j^\dagger + c_j$ and $B_j = c_j - c_j^\dagger$, i.e.,

$$\mathcal{O}^x = \lim_{r \rightarrow \infty} \langle B_2 A_3 B_3 \dots A_r B_r A_{r+1} B_{r+1} A_{r+2} \rangle. \quad (16)$$

Then, with the help of Wick theorem [55], we can go on expanding it by the contractions $\langle A_j A_l \rangle$, $\langle B_j B_l \rangle$, and $\langle B_j A_l \rangle$, whose expression can be acquired using the ground-state function. We have

$$\langle A_j A_l \rangle = \delta_{jl}, \quad (17)$$

$$\langle B_j B_l \rangle = -\delta_{jl}, \quad (18)$$

$$\begin{aligned} \langle B_j A_l \rangle &= G_{j,l} = G_r \\ &= \frac{1}{\pi} \int_0^\pi dk [\cos(kr) \cos \theta_k + \sin(kr) \sin \theta_k], \end{aligned} \quad (19)$$

where $r = j - l$. Since $\langle A_j A_l \rangle$ and $\langle B_j B_l \rangle$ are always equal to zero and by considering the characteristics of their expression,

\mathcal{O}^x can be transformed to a Toeplitz determinant,

$$\mathcal{O}^x = \lim_{r \rightarrow \infty} \begin{vmatrix} G_{-2} & G_{-3} & \cdots & G_{-r-1} \\ G_{-1} & G_{-2} & \cdots & G_{-r} \\ G_0 & G_{-1} & \cdots & G_{-r+1} \\ \vdots & \vdots & \ddots & \vdots \\ G_{r-2} & G_{r-3} & \cdots & G_{r-1} \\ G_{r-3} & G_{r-4} & \cdots & G_{r-2} \end{vmatrix}. \quad (20)$$

From the perspective of a numerical calculation, we can take finite r and calculate a finite number of integrals to obtain \mathcal{O}^x . Note that r should be as large as possible in order to approach the thermodynamic limit.

Next, we can acquire staggered magnetization at temperature T via the calculation of a spin-correlation function,

$$R_{jl}^\alpha(T) = \langle \sigma_j^\alpha \sigma_l^\alpha \rangle_T, \quad (21)$$

where α can be x , y , or z . Let us take $R_{jl}^x(T)$ as an example. Similar to the procedure of calculating the string correlation function, $R_{jl}^x(T)$ can also be expanded by $A_j = c_j^\dagger + c_j$, $B_j = c_j - c_j^\dagger$, that is,

$$\begin{aligned} R_{jl}^x(T) &= \left\langle (c_j - c_j^\dagger) \prod_{j < m < l} (1 - 2c_m c_m^\dagger) (c_l^\dagger + c_l) \right\rangle_T \\ &= \langle B_j A_{j+1} B_{j+1} \dots A_{l-1} B_{l-1} A_l \rangle_T. \end{aligned} \quad (22)$$

By using Wick theorem again, we can also convert $R_{jl}^x(T)$ into a Toeplitz determinant,

$$R_r^x(T) = \begin{vmatrix} D(-1, T) & D(-2, T) & \cdots & D(-r, T) \\ D(0, T) & D(-1, T) & \cdots & D(-r+1, T) \\ \vdots & \vdots & \ddots & \vdots \\ D(r-2, T) & D(r-3, T) & \cdots & D(-1, T) \end{vmatrix}, \quad (23)$$

where the elements of the determinant read

$$\langle B_j A_l \rangle_T = D_{jl}(T) = D(j-l, T) = D(r, T). \quad (24)$$

Similarly, $R_r^y(T)$ can be expressed by

$$R_r^y(T) = \begin{vmatrix} D(1, T) & D(0, T) & \cdots & D(-r+2, T) \\ D(2, T) & D(1, T) & \cdots & D(-r+3, T) \\ \vdots & \vdots & \ddots & \vdots \\ D(r, T) & D(r-1, T) & \cdots & D(1, T) \end{vmatrix}. \quad (25)$$

With R_r^y , we can calculate staggered magnetization m_y with the definition

$$\lim_{r \rightarrow \infty} (-1)^r R_r^y(0) = m_y^2. \quad (26)$$

Overall, with the above expression, we can investigate the influence of non-Hermiticity on the cluster Ising model's phase distribution at certain temperature.

D. Variation mode of correlation function

In phase transition theory, the spin-correlation function $R_y(r)$ decreases to a fixed nonzero value as r increases in the symmetry-breaking phase, in contrast with the exponential decay to zero in the disordered phase. At the critical point between these two phases, $R_y(r)$ exhibits a unique power-law

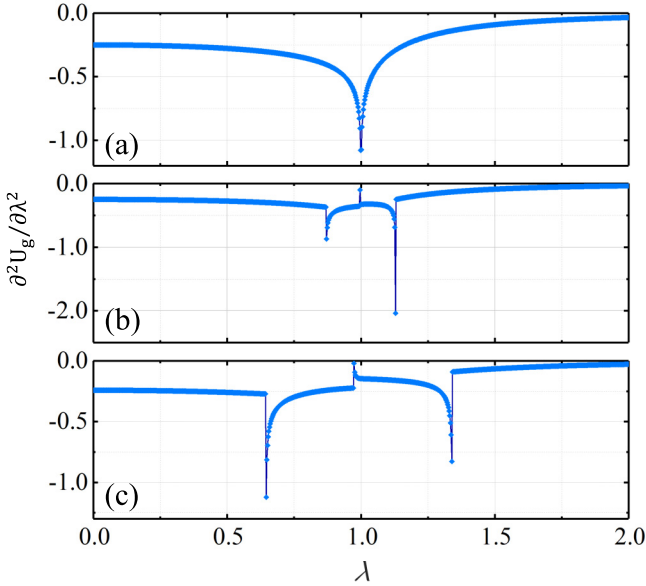


FIG. 2. The second derivative of ground-state energy density with respect to λ . (a) When $\Gamma = 0$, the singularity occurs at $\lambda = 1$, which is in good agreement with the critical point of a standard cluster Ising model. (b) When $\Gamma = 0.6$, the nonanalytical point in the Hermitian case splits into three points, indicating new potential critical points. (c) When $\Gamma = 1.6$, the distance between the three non-analytical points increases with the growing non-Hermitian strength.

decay. Similarly, the variation mode of the string order parameter $O_x(r)$ also carries the key information of the phases and phase transitions. $O_x(r)$ tends to be a constant in a nontrivial cluster phase, rather than the exponential decay in trivial phases. Moreover, it is worth mentioning that if one plots the curve of the power-law decay in the $\ln\text{-}\ln$ coordinates, it will become a straight line and the slope of the line will directly reveal one of the critical exponents η .

IV. RESULTS AND DISCUSSIONS

In this section, we are going to illustrate the influence of non-Hermiticity on different observables. Let us start with the second derivative of the ground-state energy density. In the Hermitian case, as shown in Fig. 2(a), the singularity emerges at $\lambda = 1$, which corresponds to the critical point of the standard cluster Ising model. However, when the non-Hermitian strength increases [see Figs. 2(b) and 2(c)], the singular point turns into three points, which drift apart from one another with an increasing Γ . The emergence of new nonanalytical points indicates possible new phase transitions that remain unknown. Notably, the continuous first derivative of U_g is also shown in Appendix to prove that all three of these phase transitions are continuous phase transitions.

We also demonstrate the fidelity whose singularity characterizes a phase transition as well. As is shown in Fig. 3(a), in the Hermitian case, the singular point also works well in characterizing the SPT-AFM phase transition at $\lambda = 1$. Then, we turn to the non-Hermitian cases as Γ increases to 0.6 and 1.6 [see Figs. 3(b) and 3(c)]. The behavior of singularity is in good agreement with that of $\partial^2 U_g / \partial \lambda^2$. We can observe two

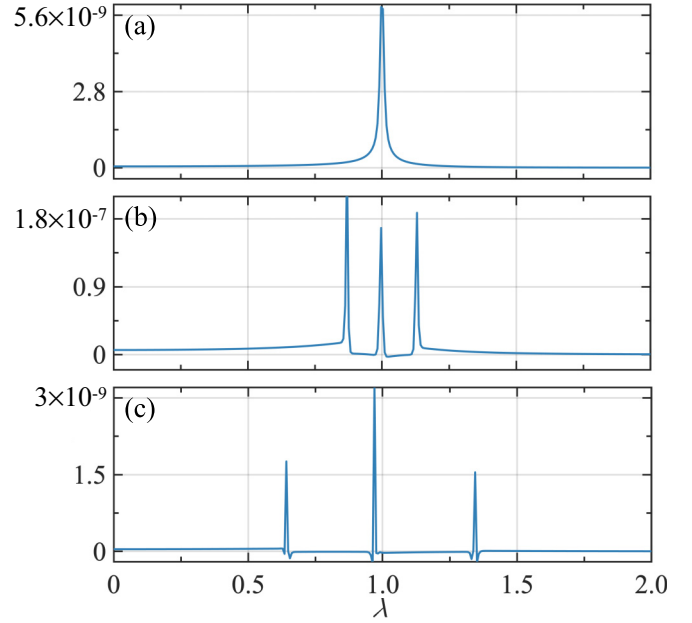


FIG. 3. The distribution of $1 - F$ (fidelity) vs λ . (a) When $\Gamma = 0$, the singular point well indicates the critical point of a conventional SPT-AFM phase transition. (b) When $\Gamma = 0.6$, the fidelity also characterizes possible new phase transition points. (c) As Γ ascends to 1.6, the behavior of singularity is the same as that of the second derivative of energy density.

more emerging singular points and witness them moving away from each other as non-Hermiticity increases, which denotes the emergence of the unknown phase transition. The results of fidelity and the second derivative of ground-state energy nicely support each other.

When one investigates the Hermitian cluster Ising model, it is a standard procedure to calculate the string order parameter O_x and staggered magnetization m_y . One can directly recognize the domination of the disordered (ordered) phase with the help of a nonlocal (local) order parameter, i.e., string order parameter (staggered magnetization), provided it is nonzero. We also investigate the distribution of these two order parameters under different non-Hermitian strengths. In the Hermitian case [see Fig. 4(a)], the behaviors of O_x and m_y are the same as the previous research, where O_x (m_y) is nonzero when $\lambda < 1$ ($\lambda > 1$) and its decline is continuous. However, when we increase the non-Hermitian strength Γ from 0 to 2, the distribution of the order parameters changes greatly. At first, on the one hand, O_x shows an intense but continuous decline after the kink at the first critical point, while on the other hand, the parameter m_y illustrates a sharp but continuous increase before the kink at the third critical point. The insets of Fig. 4(b) show the close-ups of continuous variation around the two kinks at critical points. Note that although the kinks at continuous critical points are not to be found in the Hermitian case, recent studies have proved that this kind of kink is actually a real phenomenon in the non-Hermitian case [56,57]. Thus, after involving dissipation strength, one can witness that the original two phase zones are divided into four. Then, one can see that in zones I and II, O_x is nonzero and m_y is zero. In zone IV, m_y is nonzero and O_x is

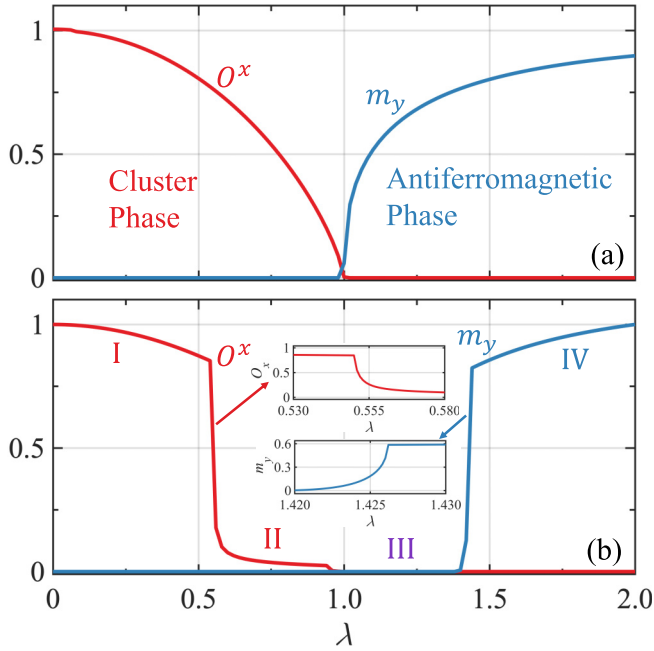


FIG. 4. The numerical results of string correlation function O_x and staggered magnetization m_y for the (a) Hermitian case with $\Gamma = 0$ and (b) non-Hermitian case with $\Gamma = 2.0$. The insets of (b) are close-ups of the continuous change region around the two phase transition points.

zero. However, in zone III, both O_x and m_y are zero, which is beyond the way of phase classification in the Hermitian case. In addition, it is noticeable that this is a numerical result where r in Eqs. (20) and (26) is taken as 1000 instead of infinite. Thus, a tiny numerical error is involved, leading to some continuous transition areas between different zones. In principle, there will be some nonanalytical slump as long

as r is large enough to approach the thermodynamics limit, the position of which is also consistent with that of singular points, as we calculated above.

From the above discussions, it is obvious that the introduction of a non-Hermitian term leads to new phases and phase transitions that transcend the framework of the Hermitian case. After that, we want to classify the emergent phases and phase transitions with the help of the variation modes of spin-correlation function $R_y(r)$ and string parameter $O_x(r)$. We investigate the variation of $O_x(r)$ and $R_y(r)$ at different λ and under different non-Hermitian strengths Γ . When $\Gamma = 0$, the critical point is at $\lambda = 1$, which denotes the cluster-AFM phase transition with symmetry breaking. From Fig. 5(a), we can see that $O_x(r)$ remains a constant value before $\lambda = 1$ and shows exponential decay to zero after $\lambda = 1$, indicating a nontrivial cluster phase and trivial AFM phase, respectively. Meanwhile, from Fig. 5(c), we can see that the curves of $R_y(r)$ before $\lambda = 1$ exhibit the exponential decay and those after $\lambda = 1$ decrease to fixed nonzero values, denoting a symmetry-protected cluster phase and symmetry-breaking AFM phase, respectively. Notably, as is shown in the insets of the two graphs, the curves at the critical point show the power-law decay, indicating the phase transition. The critical exponent η at that critical point can also be obtained as $3/4$ according to the slope of the line in the $\ln\text{-}\ln$ coordinates (natural logarithm), which is different from that of the Ising universality class. Previous work [12] also points out that although most of the critical exponents of the Hermitian cluster Ising model are equal to that of the Ising universality class, the central charge of them is different, which means the phase transition in the Hermitian cluster Ising model is beyond the Ising universality class. From our calculation, the difference in critical exponent η also provides more evidence to support the above claim.

Interestingly, as Γ increases to 2 [see Figs. 5(b) and 5(d)], exotic phases and phase transitions are revealed by the variation mode of $O_x(r)$ and $R_y(r)$. Let us start with $O_x(r)$

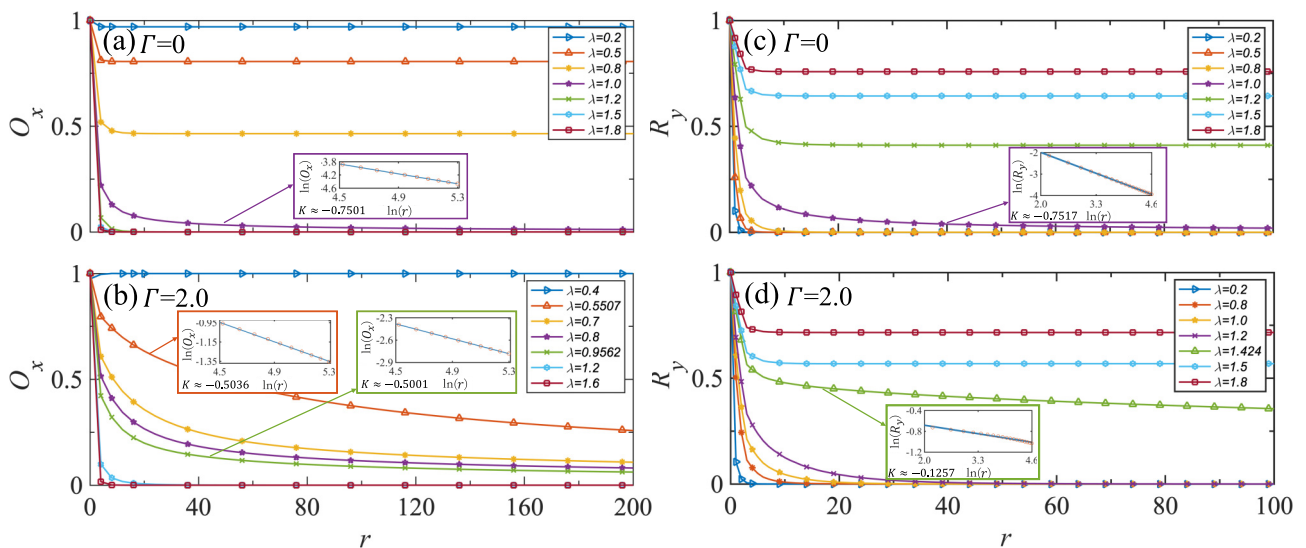


FIG. 5. The variation modes of string parameter $|O_x(r)|$ and correlation function $|R_y(r)|$ at different λ for (a),(c) Hermitian case with $\Gamma = 0$ as well as (b),(d) non-Hermitian case with $\Gamma = 2$. When $\Gamma = 0$, the insets plot the curves at critical point $\lambda = 1$ in $\ln\text{-}\ln$ coordinates and show the slope K of the lines. As Γ increases to 2, the three critical points are at 0.551, 0.956, and 1.424. The insets also show the curves featuring power-law decay in $\ln\text{-}\ln$ coordinates (with subscript e).

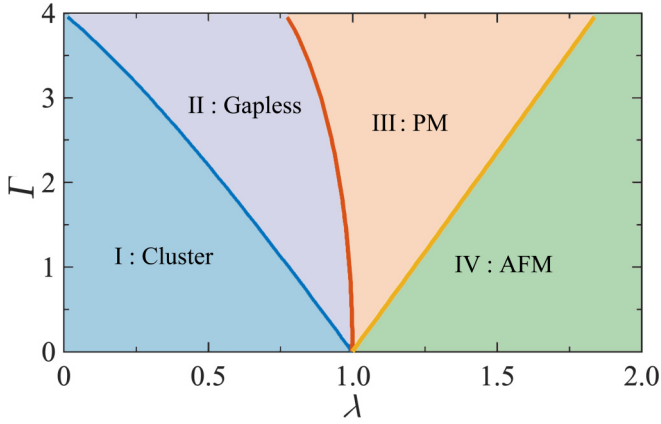


FIG. 6. The $\Gamma - \lambda$ phase diagram according to U_g 's second derivative. In the Hermitian case ($\Gamma = 0$), there is a conventional critical point of the Ising universality class at $\lambda = 1$. With the increase of Γ , the critical point splits into three critical points, denoting the phase transitions among the four different phases.

[see Fig. 5(b)]. In zone I before the first critical point, $O_x(r)$ remains a constant as string length r increases, which indicates it is a nontrivial cluster phase. In zones III and IV, $O_x(r)$ decreases exponentially to zero, which indicates they are trivial phases. However, in the whole zone II, $O_x(r)$ exhibits a power-law decay and the slope of the curves in the \ln - \ln coordinate system is close to -0.5 , which indicates that zone II is a gapless phase and the critical exponent η of the phase transitions is $1/2$. Then, let us move on to the behavior of $R_y(r)$ [see Fig. 5(d)]. One can only observe the power-law decay at the third critical point, which means that the symmetry breaking only occurs at the third phase transition. By analyzing the above two clues with the distributions of O_x and m_y shown in Fig. 4(b), we find that in zone IV, O_x is zero and AFM order parameter m_y is nonzero, which means that zone IV is a trivial AFM phase with symmetry breaking. However, both O_x and m_y are zero in zone III, which means it is a trivial phase without symmetry breaking and magnetism. Thus, it can only be a paramagnetic (PM)-AFM phase transition of the standard Ising universality class between zones III and IV. This claim is also supported by the critical exponent obtained by the slope of $R_y(r)$ at the critical point between zones III and IV: $\eta = 1/8$, which is consistent with that of the standard Ising universality class. As a result, the phase transition between zones I and II as well as zones II and III are phase transitions between a gapped phase and a gapless phase, so we call them “KT-like” phase transitions. To conclude, the introduction of the non-Hermitian term gives rise to novel phases and phase transitions as well as to the shift of critical points.

To be more comprehensive and intuitive, we investigate the $\Gamma - \lambda$ phase diagram according to the nonanalytical points of U_g 's second derivative (see Fig. 6). When $\Gamma = 0$, there is only one SPT-AFM phase transition that is beyond the Ising universality class at $\lambda = 1$. As Γ grows, the critical point extends to three consecutive critical lines. Blue, red, and yellow lines correspond to two KT-like phase transitions and a standard Ising phase transition, respectively. Notably, only the phase

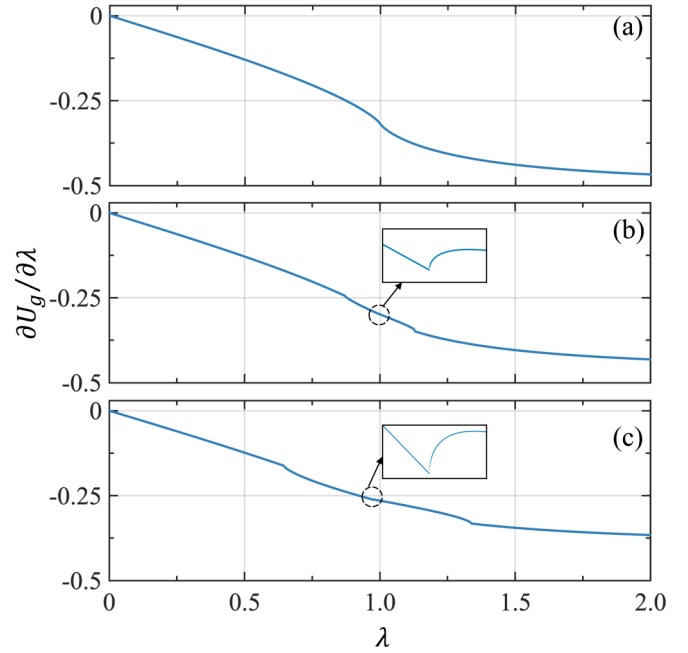


FIG. 7. The first derivative of ground-state energy density U_g under different dissipation strength Γ . (a) When $\Gamma = 0$, the distribution of $\partial U_g/\partial\lambda$ with λ . (b) When $\Gamma = 0.6$, the distribution of $\partial U_g/\partial\lambda$ with λ . (c) When $\Gamma = 1.6$, the distribution of $\partial U_g/\partial\lambda$ with λ . Insets: the zoom-in of the central area where the second critical point lies. All of the above distributions are continuous at the critical points.

transition on the yellow critical line still accompanies with the breaking of spin rotational symmetry.

V. SUMMARY

There is an SPT phase and an AFM phase in the Hermitian cluster Ising model and the phase transition between them is beyond the Ising universality class. The influence of non-Hermiticity on the cluster Ising model is investigated in this work. We first detect the singular behaviors of the second derivative of energy density and fidelity, finding that new critical points may emerge and move away from each other. Next, we numerically investigate the string order parameter and staggered magnetization, and the results show that the introduction of non-Hermiticity will give rise to a very rich phase diagram featuring phase transitions between four phases. In order to characterize them, we then investigate the variation modes of the string parameter and spin-correlation function, which help us distinguish different phases and characterize three phase transitions with the critical exponent. By combining the result of the string order parameter and staggered magnetization, the four phases are identified as a cluster phase, a gapless phase, a paramagnetic phase, and an antiferromagnetic phase, respectively. The phase transitions between them are two KT-like phase transitions and one standard Ising phase transition with the corresponding critical exponents $\eta = 1/2, 1/2$, and $1/8$, respectively. Eventually, we

give the $\Gamma - \lambda$ phase diagram to visualize the emergence and extension of the critical lines.

In the end, we briefly clarify the possible mechanism behind the novel phenomena. In the Hermitian case, when $\lambda < 1$, the SPT phase of the cluster Ising model is well protected by a $\mathbb{Z}_2 \times \mathbb{Z}_2$ symmetry, i.e., both the \mathbb{Z}_2 symmetry of σ_z 's product and the symmetry of time reversal are unbroken. However, after introducing the non-Hermitian external field, though the \mathbb{Z}_2 symmetry of σ_z 's product is intact, the time-reversal symmetry is broken, which leads to the emergence of the cluster phase in zone I, the closing of gap in zone II, as well as the emergence of the paramagnetic phase in zone III. The deeper mechanism behind the relation between the non-Hermitian external field and gapless phase remains unclear to date, which is related to the developing nonunitary conformal field theory, and we will discuss it in our future work. Our work can be realized in an ultracold atom experiment and will shed light on the experimental construction of novel phases and phase transitions in open quantum many-body systems.

ACKNOWLEDGMENTS

We thank C. X. Ding, Y. G. Liu, Q. Q. Su, M. Gong, S. Liu, and D. C. Lu for helpful discussions. This work was supported by the NSFC (Grant No. 11704132), the NSAF (Grant No. U1830111), the Natural Science Foundation of Guangdong Province (Grant No. 2021A1515012350), and the KPST of Guangzhou (Grant No. 201804020055).

APPENDIX: FIRST DERIVATIVE OF GROUND-STATE ENERGY DENSITY

To prove that all the phase transitions in the non-Hermitian case are continuous, we present the first derivative of the ground-state energy density U_g (see Fig. 7), from which one can see that the first derivative of the order parameters is continuous. Since the second derivative of U_g is discontinuous (see Fig. 2), all the phase transitions after introducing non-Hermitian dissipation are standard continuous phase transitions.

-
- [1] L. D. Landau and E. M. Lifshitz, *Statistical Physics Part 1, Course of Theoretical Physics*, Vol. 5, 3rd ed. (Butterworth-Heinemann, Oxford, 1980).
 - [2] J. M. Kosterlitz and D. J. Thouless, Ordering, metastability and phase transitions in two-dimensional systems, *J. Phys. C: Solid State Phys.* **6**, 1181 (1973)
 - [3] C. Becker, P. Soltan-Panahi, J. Kronjöger, S. Dörscher, K. Bongs, and K. Sengstock, Ultracold quantum gases in triangular optical lattices, *New J. Phys.* **12**, 065025 (2010).
 - [4] J. K. Pachos and M. B. Plenio, Three-Spin Interactions in Optical Lattices and Criticality in Cluster Hamiltonians, *Phys. Rev. Lett.* **93**, 056402 (2004).
 - [5] A. C. Doherty and S. D. Bartlett, Identifying Phases of Quantum Many-Body Systems That Are Universal for Quantum Computation, *Phys. Rev. Lett.* **103**, 020506 (2009).
 - [6] S. O. Skrøvseth and S. D. Bartlett, Phase transitions and localizable entanglement in cluster-state spin chains with Ising couplings and local fields, *Phys. Rev. A* **80**, 022316 (2009).
 - [7] Y. C. Li and H. Q. Lin, Thermal quantum and classical correlations and entanglement in the XY spin model with three-spin interaction, *Phys. Rev. A* **83**, 052323 (2011).
 - [8] X.-G. Wen, Colloquium: Zoo of quantum-topological phases of matter, *Rev. Mod. Phys.* **89**, 041004 (2017).
 - [9] F. Pollmann, E. Berg, A. M. Turner, and M. Oshikawa, Symmetry protection of topological phases in one-dimensional quantum spin systems, *Phys. Rev. B* **85**, 075125 (2012)
 - [10] Z.-C. Gu and X.-G. Wen, Tensor-entanglement-filtering renormalization approach and symmetry-protected topological order, *Phys. Rev. B* **80**, 155131 (2009).
 - [11] S. Sachdev, *Quantum Phase Transitions* (Cambridge University Press, Cambridge, MA, 1999).
 - [12] P. Smacchia, L. Amico, P. Facchi, R. Fazio, G. Florio, S. Pascazio, and V. Vedral, Statistical mechanics of the cluster Ising model, *Phys. Rev. A* **84**, 022304 (2011)
 - [13] C. X. Ding, Phase transitions of a cluster Ising mode, *Phys. Rev. E* **100**, 042131 (2019)
 - [14] W. Son, L. Amico, R. Fazio, A. Hamma, S. Pascazio, and V. Vedral, Quantum phase transition between cluster and antiferromagnetic states, *Europhys. Lett.* **95**, 50001 (2011).
 - [15] M. Popp, F. Verstraete, M. A. Martín-Delgado, and J. I. Cirac, Localizable entanglement, *Phys. Rev. A* **71**, 042306 (2005).
 - [16] L. C. Venuti and M. Roncaglia, Analytic Relations between Localizable Entanglement and String Correlations in Spin Systems, *Phys. Rev. Lett.* **94**, 207207 (2005).
 - [17] C. C. Chiang, S. Y. Huang, D. Qu, P. H. Wu, and C. L. Chien, Absence of Evidence of Electrical Switching of the Antiferromagnetic Néel Vector, *Phys. Rev. Lett.* **123**, 227203 (2019).
 - [18] V. Grigorev, M. Filianina, S. Y. Bodnar, S. Sobolev, N. Bhattacharjee, S. Bommanaboyena, Y. Lytvynenko, Y. Skourski, D. Fuchs, M. Kläui, M. Jourdan, and J. Demsar, Optical Readout of the Néel Vector in the Metallic Antiferromagnet Mn₂Au, *Phys. Rev. Applied* **16**, 014037 (2021).
 - [19] Z. Gong, Y. Ashida, K. Kawabata, K. Takasan, S. Higashikawa, and M. Ueda, Topological Phases of Non-Hermitian Systems, *Phys. Rev. X* **8**, 031079 (2018).
 - [20] K. Kawabata, K. Shiozaki, M. Ueda and M. Sato, Symmetry and Topology in Non-Hermitian Physics, *Phys. Rev. X* **9**, 041015 (2019).
 - [21] J. Li, A. K. Harter, J. Liu, L. deMelo, Y. N. Joglekar and L. Luo, Observation of parity-time symmetry breaking transitions in a dissipative Floquet system of ultracold atoms, *Nat. Commun.* **10**, 855 (2019).
 - [22] L. Li, C. H. Lee and J. Gong, Topological Switch for Non-Hermitian Skin Effect in Cold-Atom Systems with Loss, *Phys. Rev. Lett.* **124**, 250402 (2020).
 - [23] W. Chen, S. K. Özdemir, G. Zhao, J. Wiersig and L. Yang, Exceptional points enhance sensing in an optical microcavity, *Nature (London)* **548**, 192 (2017).
 - [24] B. Peng *et al.*, Parity-time-symmetric whispering-gallery microcavities, *Nat. Phys.* **10**, 394 (2014).
 - [25] A. Cerjan, S. Huang, M. Wang, K. P. Chen, Y. Chong and M. C. Rechtsman, Experimental realization of a Weyl exceptional ring, *Nat. Photon.* **13**, 623 (2019).

- [26] B. Zhen, C. Hsu, Y. Igarashi *et al.*, Spawning rings of exceptional points out of Dirac cones, *Nature (London)* **525**, 354 (2015).
- [27] Y. Wu, W. Liu, J. Geng, X. Song, X. Ye, C. K. Duan, X. Rong and J. Du, Observation of parity-time symmetry breaking in a single-spin system, *Science* **364**, 878 (2019).
- [28] C. M. Bender and S. Boettcher, Real Spectra in Non-Hermitian Hamiltonians Having PT Symmetry, *Phys. Rev. Lett.* **80**, 5243 (1998).
- [29] C. M. Bender, D. C. Brody, and H. F. Jones, Complex Extension of Quantum Mechanics, *Phys. Rev. Lett.* **89**, 270401 (2002).
- [30] C. M. Bender, Making sense of non-Hermitian Hamiltonians, *Rep. Prog. Phys.* **70**, 947 (2007).
- [31] S. Yao and Z. Wang, Edge States and Topological Invariants of Non-Hermitian Systems, *Phys. Rev. Lett.* **121**, 086803 (2018).
- [32] S. Yao, F. Song and Z. Wang, Non-Hermitian Chern Bands, *Phys. Rev. Lett.* **121**, 136802 (2018).
- [33] D. W. Zhang, Y. L. Chen, G. Q. Zhang, L. J. Lang, Z. Li and S. L. Zhu, Skin superfluid, topological Mott insulators, and asymmetric dynamics in an interacting non-Hermitian Aubry-André-Harper model, *Phys. Rev. B* **101**, 235150 (2020).
- [34] P. He, J. H. Fu, D. W. Zhang and S. L. Zhu, Double exceptional links in a three-dimensional dissipative cold atomic gas, *Phys. Rev. A* **102**, 023308 (2020).
- [35] H. Shen, B. Zhen and L. Fu, Topological Band Theory for Non-Hermitian Hamiltonians, *Phys. Rev. Lett.* **120**, 146402 (2018).
- [36] E. J. Bergholtz, J. C. Budich and F. K. Kunst, Exceptional topology of non-Hermitian systems, *Rev. Mod. Phys.* **93**, 015005 (2021).
- [37] A. Ghatak and T. Das, New topological invariants in non-Hermitian systems, *J. Phys.: Condens. Matter* **31**, 263001 (2019).
- [38] Y. He and C. C. Chien, Non-Hermitian generalizations of extended Su-Schrieffer-Heeger models, *J. Phys.: Condens. Matter* **33**, 085501 (2021).
- [39] D. W. Zhang, L. Z. Tang, L. J. Lang, H. Yan and S. L. Zhu, Non-Hermitian topological Anderson insulators, *Sci. China: Phys., Mech. Astron.* **63**, 267062 (2020).
- [40] X. W. Luo and C. Zhang, Higher-Order Topological Corner States Induced by Gain and Loss, *Phys. Rev. Lett.* **123**, 073601 (2019).
- [41] H. Jiang, L. J. Lang, C. Yang, S. L. Zhu and S. Chen, Interplay of non-Hermitian skin effects and Anderson localization in nonreciprocal quasiperiodic lattices, *Phys. Rev. B* **100**, 054301 (2019).
- [42] T. E. Lee and C.-K. Chan, Entanglement and Spin Squeezing in Non-Hermitian Phase Transitions, *Phys. Rev. X* **4**, 041001 (2014).
- [43] X. Z. Zhang and Z. Song, Non-Hermitian anisotropic XY model with intrinsic rotation-time-reversal symmetry, *Phys. Rev. A* **87**, 012114 (2013).
- [44] C. Wang, M. L. Yang, C. X. Guo, X. M. Zhao and S. P. Kou, Effective non-Hermitian physics for degenerate ground states of a non-Hermitian Ising model with \mathcal{RT} symmetry, *Europhys. Lett.* **128**, 41001 (2020).
- [45] C. Li, G. Zhang, X. Z. Zhang and Z. Song, Conventional quantum phase transition driven by a complex parameter in a non-Hermitian PT-symmetric Ising model, *Phys. Rev. A* **90**, 012103 (2014).
- [46] K. L. Zhang and Z. Song, Ising chain with topological degeneracy induced by dissipation, *Phys. Rev. B* **101**, 245152 (2020).
- [47] S. Bi, Y. He and P. Li, Ring-frustrated non-Hermitian XY model, *Phys. Lett. A* **395**, 127208 (2021).
- [48] Y. Nishiyama, Fidelity-susceptibility analysis of the honeycomb-lattice Ising antiferromagnet under the imaginary magnetic field, *Eur. Phys. J. B* **93**, 174 (2020).
- [49] Y. Nishiyama, Imaginary-field-driven phase transition for the 2D Ising antiferromagnet: A fidelity-susceptibility approach, *Physica A* **555**, 124731 (2020).
- [50] Y. G. Liu, L. Xu, and Z. Li, Quantum phase transition in a non-Hermitian XY spin chain with global complex transverse field, *J. Phys.: Condens. Matter* **33**, 295401 (2021).
- [51] N. Shibata and H. Katsura, Dissipative spin chain as a non-Hermitian Kitaev ladder, *Phys. Rev. B* **99**, 174303 (2019).
- [52] L. Pan, X. Chen, Y. Chen, and H. Zhai, Non-Hermitian linear response theory, *Nat. Phys.* **16**, 767 (2020).
- [53] M. Müller, S. Diehl, G. Pupillo, and P. Zoller, Engineered open systems and quantum simulations with atoms and ions, *Adv. At. Mol. Opt. Phys.* **61**, 1 (2012).
- [54] J. M. Zeuner, M. C. Rechtsman, Y. Plotnik, Y. Lumer, S. Nolte, M. S. Rudner, M. Segev, and A. Szameit, Observation of a Topological Transition in the Bulk of a Non-Hermitian System, *Phys. Rev. Lett.* **115**, 040402 (2015).
- [55] G. C. Wick, The Evaluation of the Collision Matrix, *Phys. Rev.* **80**, 268 (1950).
- [56] T. E. Lee, F. Reiter, and N. Moiseyev, Entanglement and Spin Squeezing in Non-Hermitian Phase Transitions, *Phys. Rev. Lett.* **113**, 250401 (2014).
- [57] B.-B. Wei and L. Jin, Universal critical behaviours in non-Hermitian phase transitions, *Sci. Rep.* **7**, 7165 (2017).